JB
Journals.ASM.org

Centromere Binding and Evolution of Chromosomal Partition Systems in the *Burkholderiales*

Fanny M. Passot,* Virginie Calderon, Gwennaele Fichant, David Lane, and Franck Pasta

Laboratoire de Microbiologie et Génétique Moléculaires, UMR 5100 CNRS/Université Paul Sabatier, Toulouse, France

How split genomes arise and evolve in bacteria is poorly understood. Since each replicon of such genomes encodes a specific partition (Par) system, the evolution of Par systems could shed light on their evolution. The cystic fibrosis pathogen *Burkholderia cenocepacia* has three chromosomes (c1, c2, and c3) and one plasmid (pBC), whose compatibility depends on strictly specific interactions of the centromere sequences (*parS*) with their cognate binding proteins (ParB). However, the Par systems of *B. cenocepacia* c2, c3, and pBC share many features, suggesting that they arose within an extended family. Database searching revealed seven subfamilies of Par systems like those of *B. cenocepacia*. All are from plasmids and secondary chromosomes of the *Burkholderiales*, which reinforces the proposal of an extended family. The subfamily of the Par system of *B. cenocepacia* c3 includes plasmid variants with *parS* sequences divergent from that of c3. Using electrophoretic mobility shift assay (EMSA), we found that ParB-c3 binds specifically to centromeres of these variants, despite high DNA sequence divergence. We suggest that the Par system of *B. cenocepacia* c3 has preserved the features of an ancestral system. In contrast, these features have diverged variably in the plasmid descendants. One such descendant is found both in *Ralstonia pickettii* 12D, on a free plasmid, and in *Ralstonia pickettii* 12J, on a plasmid integrated into the main chromosome. These observations suggest that we are witnessing a plasmid-chromosome interaction from which a third chromosome will emerge in a two-chromosome species.

Low-copy-number bacterial plasmids encode partition (Par) systems that ensure active segregation of plasmid copies prior to cell division. Most Par systems consist of three elements: an NTPase (generally ATPase), a DNA-binding protein, and a centromere. The DNA-binding protein, generically termed ParB, interacts with the centromere, *parS*, to create a partition complex. The NTPase, ParA, is recruited by the partition complexes to move sister plasmids toward opposite cell poles. There are two main types of Par system, defined according to the nature of the ATPase (21, 22). Type II, currently the best understood, has an actin-like ATPase which by forming filaments pushes sister plasmids to the poles (7, 41). Type I, the most common, has a P-loop ATPase (45) which oscillates over the nucleoid (9, 26) and, at least *in vitro*, polymerizes (3, 6). How these ParA proteins segregate plasmids remains speculative.

Type I ParA and ParB proteins are diverse in sequence (5), but their genetic organization falls mostly into two subtypes: Ia (e.g., plasmids F and P1) and Ib (e.g., plasmids pTAR, TP228, and pB171-Par2) (21). Ia ParA proteins are large (Table 1), with an N-terminal extension that binds the promoter to regulate the *parAB* operon, while Ib ParA proteins are small and have no promoter-binding domain. Ia ParB proteins bind the centromere via a helix-turn-helix (HTH) domain. Ib ParB proteins are small and bind via a ribbon-helix-helix domain to a centromere which harbors the *parAB* promoter (48). More recently, type III and IV partition systems have been identified. The type III systems drive partition with tubulin-like GTPases, whereas the type IV systems use a single, non-NTPase coiled-coil protein (33, 49–51).

Most bacterial chromosomes also encode Par systems, but the role of these in chromosome partitioning is often unclear. Their contribution may be evident only for cells in certain physiological states, such as growth deceleration in *Pseudomonas putida* and sporulation in *Streptomyces coelicolor* (23, 32); it may be restricted in scope, e.g., to positioning of new *oriC* replicas (34, 47, 52), and it may be indirect, as in regulation of the replication initiator DnaA (30, 44) and of the DNA condensin SMC (24). Nevertheless, chromosomal Par systems are true partitioning machines, since they can stabilize plasmids (15, 23, 56). Chromosomal Par systems constitute a specific subtype of type I (21, 56). Their ParA proteins have no N-terminal extension, like Ib ParA proteins, while their ParBs are large, with a central HTH domain (37), like Ia ParB proteins. Unlike plasmid centromeres, which are highly variable (Table 1) and located next to their *parAB* genes, chromosomal *parS* units are 16-bp palindromes of remarkably uniform ("universal") sequence (38), dispersed within the region surrounding the replication origin (4, 39).

Although bacteria typically possess a single chromosome, some have more than one, notably proteobacteria in the orders *Vibrionales*, *Rhodobacterales*, *Rhizobiales*, and *Burkholderiales*. Split genomes are organized in a characteristic pattern: the largest chromosome has most of the housekeeping genes, an *oriC*, and a Par system similar to those of monochromosome species; secondary chromosomes have fewer housekeeping genes, a plasmid-like *oriC*, and a specific Par system (15, 17). The last feature suggests a crucial role for Par systems in the maintenance of multichromosome genomes.

One such genome is that of *Burkholderia cenocepacia* ET12, a bacterium of soils and roots also identified as an aggravating agent in cystic fibrosis (28). The first ET12 isolate to have its genome

Received 24 March 2012 **Accepted** 15 April 2012

Published ahead of print 20 April 2012

Address correspondence to Franck Pasta, pasta@ibcg.biotoul.fr.

* Present address: Fanny M. Passot, Institut de Génétique et Microbiologie, UMR 8621 CNRS/Université Paris-Sud 11, Orsay, France.

Supplemental material for this article may be found at http://jb.asm.org/.

doi:10.1128/JB.00041-12

TABLE 1 Features of *par* loci of *B. cenocepacia* J2315 replicons and other model systems[a]

Replicon	ATPase (avg residues)	DNA-binding protein (avg residues)	Minimal centromere repeat	Reference(s)
Universal chromosome	ParA (250–270)[b]	ParB (280–330)[b]	tGTTNCACGTGAAACa[c]	38
J2315 c1	ParA (259)	ParB (305)	TGTTTCACGTGAAACa	15
J2315 c2	ParA (220)	ParB (353)	gTTTATGCGCATAAAc	15
J2315 c3	ParA (231)	ParB (343)	gTTGTCACGTGACAAc	15
J2315 pBC	ParA (223)	ParB (290)	cTTGGCTCGAGCCAAg	15
Ralstonia c2	ParA (222)	ParB (334)	cTTTCAGCGCTGAAAg	15, 39
Plasmid RK2	IncC (364–259)[d]	KorB (358)	TTTAGCSGCTAAA	2
Vibrio c2	ParA (407)	ParB (323)	NTTTACANTGTAAAN	39, 57
Phage P1 (Ia)	ParA (398)	ParB (333)	(A) ATTTCAM (B) TCGCCA[e]	12, 19
Plasmid F (Ia)	SopA (391)	SopB (323)	TGGGACCACGGTCCCA	43
Rhizobiales MP	RepA (400–435)[b]	RepB (300–370)[b]	GTTNNCNGCNGNNAAC[c]	10
Plasmid TP228 (Ib)	ParF (206)	ParG (76)	ACTCWWWW	18, 55
Plasmid pTAR (Ib)	ParA (222)	ParB (94)	AYCCGRT	18, 20
Plasmid pB171 (Ib)	ParA (214)	ParB (91)	TTATKA	16, 18

[a] c1, c2, c3, and MP refer to chromosomes 1, 2, and 3 and to megaplasmids, respectively; Ia and Ib are Par system subtypes. Convergent arrows indicate symmetry. The single letter code is as follows: N = A, C, G, or T; S = C or G; M = A or C; W = A or T; Y = C or T; R = A or G; and K = G or T. Lowercase letters indicate bases that vary in the few natural repeats detected.
[b] Size range of proteins in this category.
[c] Consensus based on different replicons of the category.
[d] Full and N-terminus-lacking forms of IncC.
[e] (A) and (B) refer to the A and B boxes of P1 centromere.

sequenced, J2315 (27), has three chromosomes (c1 to c3, defined as carrying essential genes), of 3.9, 3.2, and 0.9 Mb, and a plasmid of 93 kb (pBC). Although the *par* loci of all four replicons are strictly specific with regard to partition (15), those of the secondary chromosomes, c2 and c3, and the plasmid pBC are very similar with respect to protein size, clustering of *parS* sites upstream of *parAB*, and, more strikingly, the structure of *parS* (Table 1) (15, 39). These similarities suggest evolution from a common ancestor, within either *B. cenocepacia* or its predecessors. The *in silico* analysis of bacterial genomes we report here strengthens this hypothesis by revealing a distinct set of *B. cenocepacia*-like partition systems, all on secondary chromosomes and plasmids of the wider *Burkholderiales* group. To further characterize a link between these Par systems, we explored the possibility of so-far-undetected cross-reactions between ParB proteins and noncognate *parS* sites of related species. The cross-reactions we found suggest that extant Par systems indeed retain the capacity to bind centromeres of their family despite high DNA sequence divergence.

MATERIALS AND METHODS

***In vivo* determination of *parS*-induced growth inhibition.** *parS* sites of J2315 and mutated derivatives were obtained by annealing two oligonucleotides (Eurogentec) complementary at the 3′ end but carrying at the 5′ end either an EcoRI or an MluI overhang. The duplex was cloned between the EcoRI and MluI sites of the broad-host-range, multicopy, Cm^r vector pMMB206 (42). $parS^+$ c2 and $parS^+$ pBC clusters were obtained by PCR amplification of J2315 genomic DNA. PCR fragments were cut with ApaI and HindIII or ApaI and HpaI and cloned in pMMB206 similarly cut. Recombinant plasmids were introduced into the J2315 derivative strain Mex1 by electrotransformation as described previously (14). Cells were spread on LB agar with chloramphenicol (40 μg/ml) and incubated at 37°C. From day 2 to day 7, colonies were scored twice a day.

Sources of *Burkholderiales* ParB proteins. The sources of the *parB* genes were *Burkholderia cenocepacia* J2315 (DSMZ), *Burkholderia vietnamiensis* G4 (J. Tiedje, Michigan State University), *Polaromonas naphthalenivorans* CJ2 (DSMZ), *Polaromonas* sp. strain JS666 (ATCC), *Ralstonia pickettii* 12D and 12J (T. Marsh, Michigan State University), *Ralstonia solanacearum* GMI1000 (M. Arlat, INRA, Toulouse, France), and *Rhodoferax ferrireducens* DSM 15236 (D. Lovley, University of Massachusetts).

ParB cloning and extract preparation. Wild-type *parB* genes of J2315 and other *Burkholderiales* were amplified by PCR from start to stop codon on genomic DNA. Primers were designed with a consensus Shine-Dalgarno sequence inserted 7 bp upstream of the start codon. *parB* genes were inserted under the control of the *pBad* promoter into the pDAG127 vector (35) with a deletion of the *sopA* gene by NheI/HindIII or EcoRI/HindIII digestion. Directed mutagenesis of the putative HTH of *B. cenocepacia* J2315 c3 and *Ralstonia pickettii* 12D plasmid 1*parB* genes in pDAG127 was ordered from GenScript. Recombinant plasmids, verified by sequencing, were electroporated into the *Escherichia coli* strain DLT812 (36). Cells grown in LB medium at 37°C to an optical density at 600 nm (OD_{600}) of 0.25 were induced with 0.1% arabinose (final concentration), incubated for 4 h at 37°C, and chilled on ice for 10 min. Subsequent steps were carried out at 4°C. Cells were centrifuged, washed with TNE (50 mM Tris-HCl [pH 7.5], 50 mM NaCl, 1 mM EDTA), and resuspended in TNES (TNE, 20% sucrose) at an OD_{600} of 300. Lysozyme was added at 400 μg/ml; cells were then incubated for 5 min, frozen with liquid nitrogen,

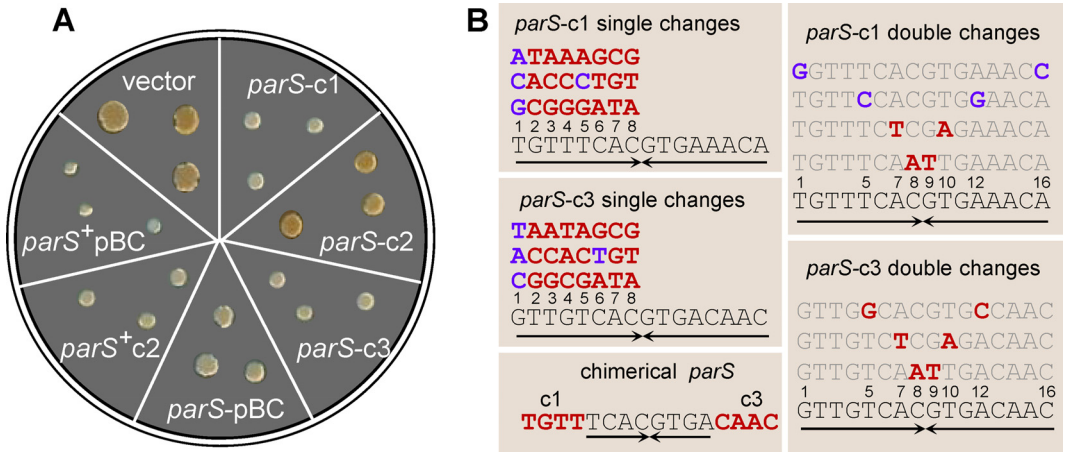

FIG 1 Extra *parS* sites inhibit growth in *B. cenocepacia* J2315. (A) Growth inhibition induced by wild-type *parS* sequences. Each sector shows three colonies of J2315-Mex1 4 days after transformation with the pMMB206 vector or recombinant derivatives carrying *parS*-c1, -c2, -c3, or -pBC in single copy or the *parS*-c2 and -pBC clusters (denoted *parS*$^+$). (B) Mutated *parS*-c1 and *parS*-c3 sequences tested for growth inhibition. Each single-base change in *parS*-c1 and *parS*-c3 (left top and middle boxes) is shown above its corresponding wild-type base (numbered), in blue when silent (i.e., still growth inhibitory) or in red when leading to loss of function (i.e., allowing normal growth). Doubly mutated *parS*-c1 and *parS*-c3 (right boxes) are shown above the wild-type sequence, with changed bases in blue or red as described above. The chimeric *parS*-c1/c3 sequence, a loss-of-function mutant, is shown (bottom left), with the noncomplementary *parS*-c1 and *parS*-c3 ends indicated in red. Arrows, inverted repeated sequences.

and thawed on ice. Lysis buffer (TNES, 660 mM NaCl, 4.5 mM dithiothreitol) was added to bring the OD_{600} to 200, the mixture was incubated on ice for 10 min, and the cells were lysed by sonication. The lysate was centrifuged for 15 min at 10,600 × *g* and the supernatant centrifuged at 20,800 × *g*. The final supernatant was then frozen with liquid nitrogen and stored at −20°C. Total protein concentrations were measured using the Bradford method (Bradford protein assay; Bio-Rad). Samples containing 3.5 μg of protein were electrophoresed in 4 to 12% polyacrylamide bis-tris denaturing gels (NuPage; Invitrogen) at a constant voltage of 200 V for 55 min and then stained with a Coomassie blue derivative (InstantBlue Expedeon) for estimation of ParB concentration.

Electrophoretic mobility shift assays (EMSA). *parS* DNA probes obtained by annealing 26-base oligonucleotides (PAGE purified by Sigma) were ^{32}P labeled using T4 polynucleotide kinase. Total protein extracts of *E. coli* (0.2 to 25 μg for initial titration tests and 10 μg for subsequent tests) were added to the probes (1 nM in 50 mM Tris-HCl [pH 7.5], 100 mM NaCl, 10% glycerol) on ice and then incubated for 10 min at room temperature prior to electrophoresis on 5% polyacrylamide gels in TBE buffer (90 mM Tris-borate, 1 mM EDTA) at 160 V for 2 h at 4°C. The gels were dried on Whatman DE81 paper and exposed to a PhosphorImager screen (Fuji). Proportions of shifted and unshifted probes were measured using the MultiGauge program (Fujifilm).

Bioinformatic analysis. For detection of *parS* motifs, defined 14-bp palindromic sequences with a central CG were first used as queries at NCBI/BLAST, with the program adapted for short, nearly exact matches of the blastn suite on all bacterial genome sequences. A second analysis was carried out using the proteins ParA and ParB encoded by chromosome 2 of *Ralstonia eutropha* as queries to perform similarity searches with the BLASTP2 program of the BLAST suite (1). The search was carried out on all protein sequences deduced from the genome annotations of completely sequenced *Burkholderiales* genomes (chromosomes and plasmids) downloaded from the EBI site (http://www.ebi.ac.uk/genomes/) and incomplete genomes from the NCBI (http://www.ncbi.nlm.nih.gov/). The vicinity of *parAB* loci was explored using PatScan (13) for the presence of palindrome motifs of at least 14 bp with a central CG, with one mismatch allowed.

Multiple alignment was generated with MAFFT (31) and edited with Jalview (54). A maximum likelihood tree was generated with PhyML (25), using the JTT amino acid substitution model of evolution (29), four categories of substitution rate, and 1,000 bootstrap replicates. Tree topology, branch length, and substitution rate parameters were optimized. The tree was rooted using NJplot (46), drawn using Treedyn (11), and colored according to ParB subfamilies. Comparisons between chromosome 1 from *Raltonia pickettii* 12J and plasmid 2 from *Ralstonia pickettii* 12D sequences were performed with the Artemis Comparison Tool (8) (http://www.sanger.ac.uk/Software/ACT).

RESULTS

ParB/centromere selectivity in *B. cenocepacia* J2315. When expressed in *E. coli*, the *parAB* operons of *Burkholderia cenocepacia*—c1, c2, c3, and pBC—each stabilize only the mini-F vector that carries its cognate *parS* (15), implying strict ParB/*parS* specificity. Nevertheless, similarities among the *parS* sites of the four replicons (Table 1) suggest some potential for cross-reaction.

To investigate ParB-*parS* interactions in the natural host, we transformed *B. cenocepacia* with plasmids carrying each of the *parS* sites. Ability to bind ParB would provoke competition with native centromeres, which could well impair growth. Indeed, transformant colonies appeared later than those of cells transformed by the vector alone. The colony size 4 days after transformation is very reproducible and thus a sensitive indicator of growth impairment. In the case of c2 and pBC, the whole *parS* cluster (i.e., 5 and 3 *parS* sites, respectively; see operon structures in Fig. 3) was required for clear inhibition, whereas for c1 and c3 a single *parS* site was sufficient (Fig. 1A). We took advantage of the latter high sensitivity to assay the effects of all single base substitutions on one arm of the 16-bp palindromes *parS*-c1 and *parS*-c3 (Fig. 1B). In *parS*-c1 most single changes lead to loss of function, i.e., unperturbed growth of transformant colonies, whereas substitutions at position 1 and the transition T5C do not, i.e., maintenance of growth inhibition. Mutant *parS*-c1 sites with symmetric double changes at these positions remained partly (T1G-A16C) or fully (T5C-A12G) inhibitory for growth. Among *parS*-c3 mutants, those with changes at position 1 or the transition C6T imparted a degree of inhibition, the others none. As the 8-bp core sequences of *parS*-c1 and -c3 are identical, we tested a hybrid

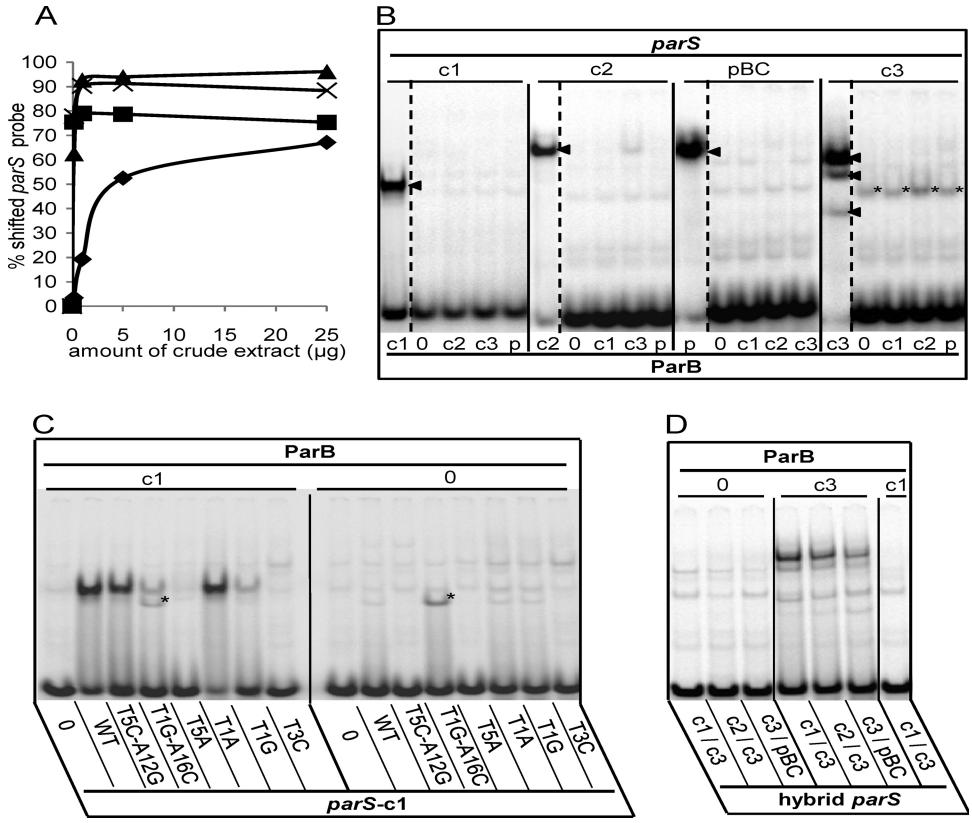

FIG 2 EMSA of the Par systems of *B. cenocepacia*. (A) Binding of each *B. cenocepacia parS* probe was tested with increasing amounts (0.2, 1, 5, and 25 μg) of crude extracts of *E. coli* cells overproducing its cognate ParB (▲, c3; ×, pBC; ■, c2; ◆, c1). (B) Radiolabeled *parS* probes, denoted above each group of lanes, were incubated with 10 mg of crude extract protein containing ParB-c1 (lanes c1), -c2 (lanes c2), -c3 (lanes c3), or -pBC (lanes p) or no ParB (lanes 0). The cognate ParB-*parS* interactions produce a single shifted complex in the case of c1, c2, and pBC and a three-band pattern in the case of c3 (arrowheads). The *parS*-c3 fragment is also retarded by an unknown *E. coli* protein (*). (C) Protein extracts containing ParB-c1 or no ParB, indicated by "c1" and "0" above the lane groups, were incubated with the radiolabeled 26-bp probes indicated below each lane as follows: negative-control sequence CTAGTCGTACGACTAG (lanes 0), wild-type *parS*-c1 (lanes WT), and *parS*-c1 mutated as indicated (other lanes). The mutated *parS*-c1 T1G-A16C fragment is shifted by an unknown *E. coli* protein (*). (D) Cell extracts containing no ParB, ParB-c3, or ParB-c1 (as indicated) were incubated with the hybrids indicated below each lane.

parS-c1/c3 (Fig. 1B). This sequence was not inhibitory, i.e., it did not compete *in vivo* with either *parS*-c1 or *parS*-c3.

To complement these results, we carried out electrophoretic mobility shift assays (EMSA) using short duplex *parS* probes and extracts of ParB-overproducing *Escherichia coli* cells (see Materials and Methods). Extracts were used rather than purified ParB proteins, owing to the impracticability of purifying certain proteins which, despite strong transcription of their genes, could be obtained only at low concentrations. Because of variation of ParB concentrations between extracts (see Fig. S1 and Table S1 in the supplemental material), we determined the quantities of extract appropriate for EMSA by measuring the binding of each *parS* probe as a function of the quantity of extract protein containing the cognate ParB (Fig. 2A). For ParB-c2, -c3, and -pBC, 1 μg of extract gave maximal binding. For ParB-c1, >5 μg was required for a strong binding, even though this was the most concentrated of the ParB proteins. Variation in intrinsic affinity and in the active fraction of each ParB presumably accounts for the differences in binding efficiency. We carried out further EMSA using 10 μg for all ParB proteins, which ensures strong binding of the four ParB homologues to their cognate probes. Figure 2B shows that even at these higher-than-saturating ParB concentrations, each *parS* bound only its cognate ParB. For *parS*-c1, -c2, and -pBC, binding produced a single retarded species. In the case of *parS*-c3, three bands appeared. Although the two faster-migrating bands might be due to cleavage products of ParBc3, other explanations have not been ruled out (see the legend to Fig. 6).

We then examined the binding of ParB-c1 and ParB-c3 to mutant *parS*-c1 sites. Mutant *parS*-c1 that no longer inhibited growth also failed to bind ParB-c1, as illustrated by T5A and T3C (Fig. 2C), while those that did inhibit growth, such as T1A and T1G, still bound (Fig. 2C). The noninhibitory hybrid *parS*-c1/c3 also failed to bind ParB-c1 (Fig. 2D). Binding affinities reflected relative *in vivo* inhibition in some cases (compare T5C-A12G with T1G-A16C in Fig. 2C) but not all (T1A and T1G mutants appeared equally inhibitory). In contrast, ParB-c3 exhibited distinct binding properties; e.g., the hybrid sequence *parS*-c1/c3, although noninhibitory, bound ParB-c3 with somewhat reduced affinity, forming the characteristic three-band pattern (Fig. 2D), as did two other chimerae not tested *in vivo*, c2/c3 and c3/pBC (Fig. 2D; see Table 1 and Fig. 3 for *parS* sequences). *In vitro* binding of ParB-c3 appears to tolerate changes in one arm of the cognate sequence. This result appears to be at odds with the *in vivo* tests, in which most changes in one arm of *parS*-c3 abolished inhibition. *In vivo*, however, *parS* sites entering on a plasmid compete for ParB with chromosomal *parS* sites. Moreover, an entering single *parS*-c3 site

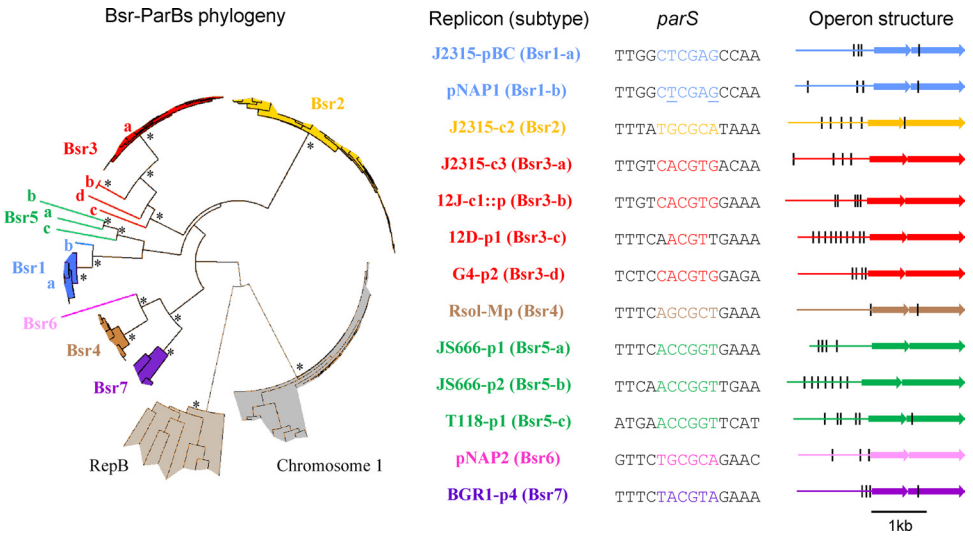

FIG 3 Bsr families and corresponding *parS* palindromes. Each color corresponds to one of the seven Bsr families. ParB proteins and loci are listed in Table S1 in the supplemental material. For clarity, only the bootstrap values superior to 800 concerning the deep branches are indicated (*). RepB proteins from *Rhizobiales* megaplasmids and chromosome 1 ParB proteins from *Burkholderiales* are indicated as outgroups. Protein and *parS* variations allow identification of 13 Bsr subtypes. Each subtype is exemplified (right) by one replicon: *B. cenocepacia* J2315 plasmid pBC (J2315-pBC), *B. cenocepacia* J2315 chromosome 2 (J2315-c2), *B. cenocepacia* J2315 chromosome 3 (J2315-c3), *P. naphthalenivorans* CJ2 plasmid 1 (pNAP1), *P. naphthalenivorans* CJ2 plasmid 2 (pNAP2), plasmid integrated in chromosome 1 of *R. pickettii* 12J (12J-c1::p), *R. pickettii* 12D plasmid 1 (12D-p1), *B. vietnamiensis* G4 plasmid 2 (G4-p2), *R. solanacearum* GMI 1000 megaplasmid (Rsol-Mp), *Polaromonas* sp. strain JS666 plasmid 1 (JS666-p1), *Polaromonas* sp. strain JS666 plasmid 2 (JS666-p2), *R. ferrireducens* T118 plasmid 1 (T118-p1), and *Burkholderia glumae* BGR1 plasmid 4 (BGR1-p4). The minimal 14-bp palindrome (*parS*) near the *parAB* operon is indicated. In the case of pNAP1 *parS*, underlined letters indicate positions of degeneracy. The structure of each *parAB* operon is shown (black line, minimal palindrome; first arrow, *parA*; second arrow, *parB*). ParA proteins vary from 217 residues (BGR1-p4) to 242 (JS666-p2), and ParB proteins vary from 290 (J2315-pBC) to 376 (JS666-p2).

must compete with a natural cluster of *parS* sites that binds ParB more strongly (15). Correspondence between the *in vivo* test and EMSA with ParB-c3 nevertheless appears: e.g., C6T is the only internal mutant that maintains the inhibition, and accordingly, the double symmetric mutant C6T-G11A is the only one to show ParB binding comparable to that of the wild type (see Fig. 5).

These results confirm that ParB/*parS* systems of *B. cenocepacia* are highly specific and nonoverlapping. Some relaxation of specificity is nevertheless possible, suggesting that certain of these systems might cross-react with those of related bacteria.

Par families characteristic of secondary replicons of *Burkholderiales*. We carried out a bioinformatic analysis of available eubacterial genomes to find centromeres similar to those of J2315. The criteria were (i) palindromes of at least 14 bp, (ii) a central CG dinucleotide, (iii) a T-rich 5′ end, and (iv) a location upstream of a *parAB* operon. We found such palindromes. In all cases, the adjacent *parAB* genes encode proteins with sizes similar to those of J2315 (Fig. 3). These loci were found only in species from the order *Burkholderiales*, most of them belonging to the family *Burkholderiaceae* (genera *Ralstonia*, *Cupriavidus*, and *Burkholderia*) and five to *Comamonadaceae* (genera *Polaromonas* and *Rhodoferax*). Essentially all these loci are in secondary chromosomes or large plasmids. The one apparent exception is a *par* locus on chromosome 1 (c1) of *Ralstonia pickettii* 12J; however, it appears to belong to a 380-kb plasmid integrated in the terminus region of c1. We identified 8 new palindromic *parS* motifs related to those of *B. cenocepacia*. On the basis of the phylogenies and the *parS* sequences, we could distinguish seven families of *par* loci, which we name Bsr (*Burkholderiales* secondary replicon) (Fig. 3). Bsr1 is the Par family of the plasmid pBC (15), and most Bsr1 ParB proteins are from *Burkholderia* plasmids, forming a narrow cluster (Bsr1-a [Fig. 3]). One Bsr1 ParB, more divergent, corresponds to the plasmid pNAP1 of *Polaromonas naphthalenivorans* CJ2 (Bsr1-b [Fig. 3]). Bsr1 members share the *parS* TTGGCTCGAGCCAA, but the pNAP1 *parS* set includes variants with a one-base transversion, T6G or G10T. Bsr2 is the family to which chromosome 2 *parAB* loci of *Burkholderia* species belong. Bsr3 consists mostly of a narrow cluster with a defined *parS* (Bsr3-a [Fig. 3]). This *parS* and the associated *par* genes appear characteristic of chromosome 3 of closely related species which together compose the *Burkholderia cepacia* complex (Bcc) (40, 53) rather than of *Burkholderia* in general. Three other Bsr3 ParB subtypes were found, each associated with a specific *parS* motif (Bsr3-b, -c, -d [Fig. 3]). Bsr4 is the family of Par systems of *Ralstonia-Cupriavidus* megaplasmid chromosome 2, previously identified (15, 39). Bsr5, Bsr6, and Bsr7 are novel. Bsr5 groups three *Comamonadaceae* plasmid Par systems whose *parS* sites share the core sequence ACCGGT. Bsr6 is defined by the Par system of plasmid 2 of *Polaromonas naphthalenivorans* CJ2. Bsr7 groups the *par* loci of *Burkholderia glumae* BGR1 plasmid 4 and some of the unassembled contigs of *Burkholderia* species (see Table S2 in the supplemental material).

ParB-*parS* cross-reactions within Bsr families. The Bsr families with variant *parS* sites and ParB proteins appeared well suited to addressing the question of whether ParB proteins bind natural noncognate centromeres. The *parB* genes of representatives of Bsr families 1 to 6 and their subfamilies (Fig. 3) were amplified, cloned, and expressed in *E. coli*, and the ParB proteins in cell extracts were tested by EMSA for binding to various *parS* sites. All ParB/*parS* cognate shifts were detected (Fig. 2 and 4; see also Fig. S2 in the supplemental material) except for the three plasmids of the Bsr5 family whose poor ParB protein solubility precluded analysis.

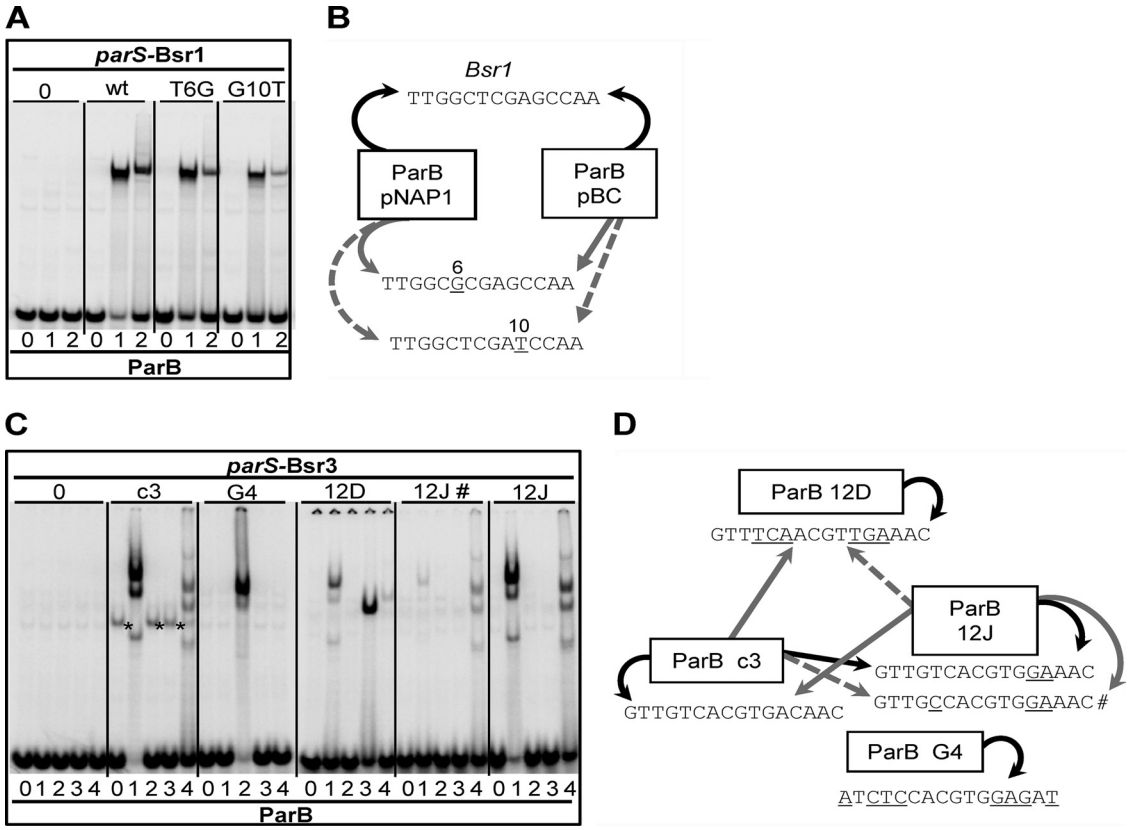

FIG 4 Cross-reactions in Bsr1 and Bsr3 families. (A) EMSA of Bsr1 ParB proteins and *parS* sites. Samples are grouped according to *parS*, indicated below: 0, negative-control sequence TAGTCGTACGACTA; wt, *parS* Bsr1, TTGGCTCGAGCCAA, common to pBC (Bsr1-a) and pNAP1 (Bsr1-b); T6G and G10T, *parS* derivatives exclusive to pNAP1. ParB proteins are denoted above *parS* as follows: 0, no ParB; 1, ParB-pBC; 2, ParB-pNAP1. (B) Bsr1 interaction summary. Arrows indicate that ParB in the box binds the *parS* pointed to. Curved and straight arrows represent cognate and noncognate binding, respectively. Black, gray, and dashed arrows correspond, respectively, to strong, medium, and weak binding relative to the specific binding. pNAP1-*parS* sequences are shown with bases changed relative to *Bsr1* underlined and numbered. (C) EMSA of Bsr3 ParBs and *parS* sites. Samples are grouped according to *parS*: 0, negative-control sequence CTAGTCGTACGACTAG; c3, *parS* chromosome 3; G4, *parS* plasmid 2 of *B. vietnamiensis* G4; 12D, *parS* plasmid 1 of *R. pickettii* 12D; 12J #, secondary *parS* of *R. pickettii* 12J; 12J, main *parS* of *R. pickettii* 12J. ParB proteins are denoted as follows: 0, no-ParB extract; 1, ParB-c3; 2, ParB-G4; 3, ParB-12D; 4, ParB-12J. The *parS*-c3 fragment is also retarded by an unknown *E. coli* protein (*). (D) Bsr3 interaction summary. Arrows signify interactions as described for panel B. *parS* sequences are shown below each box, with bases changed relative to *parS*-c3 underlined.

We then sought cross-reactions between and within families whose *parS* elements shared sequence similarity. None were found among the Bsr2, Bsr4, and Bsr6 families (Fig. S2 in the supplemental material). On the other hand, the Bsr1 ParB of pBC bound not only to the *parS* characteristic of its family but also to the two variant *parS* sites specific to the Bsr1-b locus of pNAP1. Moreover, the pNAP1 and pBC ParB proteins showed the same order of affinity for the three *parS* sites: wild type > T6G > G10T (Fig. 4A and B). This result confirms the phylogenic link between the two ParBs and suggests that the changes in the *parS* sites of pNAP1 affect bases not essential for binding of these proteins.

Cross-reaction was also found in Bsr3. This result was more surprising because proteins and *parS* sites of this family exhibit considerable divergence. The main subtype (Bsr3-a [Fig. 3]) is that of *B. cenocepacia* J2315 chromosome 3 (c3). The other subtypes, i.e., Bsr3-b, -c, and -d (Fig. 3), are from, respectively, (i) a plasmid integrated into chromosome 1 of *Ralstonia pickettii* 12J (referred to as 12J; this system is also found on plasmid 2 of *Ralstonia pickettii* 12D), (ii) plasmid 1 of *Ralstonia pickettii* 12D (referred to as 12D), and (iii) plasmid 2 of *Burkholderia vietnamiensis* G4 (referred to as G4).

Cross-recognition between these subtypes was tested by EMSA (Fig. 4C and D). ParB-c3 bound the incomplete palindromic *parS*-12J almost as strongly as its own *parS* and more strongly than the nonpalindromic hybrid *parS* sites shown in Fig. 2D. Reciprocally, ParB-12J bound *parS*-c3 strongly. Also, both proteins formed a multiband pattern, further implying their relatedness. There are nevertheless obvious differences in the binding specificities of these proteins; e.g., (i) binding to the T5C variant of *parS*-12J (*parS*-12J# in Fig. 4C and D) was scarcely detected, whereas ParB-12J showed significant binding; (ii) ParB-c3 bound *parS*-12D better than ParB-12J did; and (iii) unlike *parS*-c3, *parS*-12J was not inhibitory when introduced into *B. cenocepacia*.

ParB-c3 bound to *parS*-12D, which was surprising given that *parS*-12D diverges from *parS*-c3 by three substitutions in each arm: G4T, T5C, and C6A and, symmetrically, C13A, A12G, and G11T. Bsr7-*parS* (Fig. 3) differs from *parS*-c3 by the same substitutions as *parS*-12D except with C6T-G11A instead of C6A-G11T. However, Bsr7-*parS* was bound by ParB-c3 very weakly (Fig. 5), which led us to examine the role of each of the symmetrical base change pairs in determining binding of ParB-c3 (Fig. 5). By itself, T5C-A12G, common to *parS*-12D and *parS*-Bsr7, drastically re-

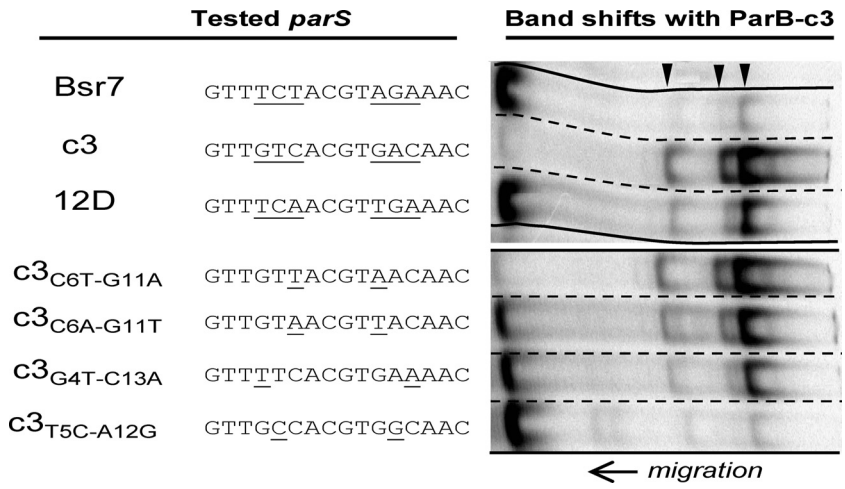

FIG 5 Binding of ParBc3 to *parS*-c3, *parS*-12D, *parS*-Bsr7, and related or mutated sequences was analyzed by EMSA. Positions 4, 5, and 6 and 11, 12, and 13 are underlined in *parS*-c3. Underlined bases in the other *parS* sequences differ from those in *parS*-c3. The characteristic three-band pattern of ParB-c3 is indicated by arrowheads.

duced binding. G4T-C13A, also common to both *parS* sites, allowed moderate binding. C6T-G11A, exclusive to *parS*-Bsr7, allowed binding comparable to that of the wild type, and C6A-G11T, exclusive to *parS*-12D, allowed strong binding. It appears that *parS*-12D is bound by ParB-c3 specifically despite its differences from *parS*-c3, which include even the detrimental T5C-A12G double change.

Identification of a domain involved in specific binding. The foregoing results show that *in vitro*, ParB-c3 binds different *parS* motifs of the Bsr3 family, notably *parS*-12D, while ParB-12D fails to bind *parS*-c3. What are the determinants responsible for such differences? Typically, a helix-turn-helix (HTH) constitutes the core of the DNA-binding domain of ParB proteins. The prediction of an HTH motif for ParB-c3 was weak (15), and we have found this to be so for the other Bsr3-ParB subtypes. Nevertheless, protein alignments revealed amino acid conservation in the region where most ParB proteins have a putative or verified HTH domain. Moreover, certain observations are compatible with the assignment of DNA recognition and binding to this region of ParB: (i) mutation of the highly conserved Ala5 of helix 1 (Fig. 6A) reduced binding of ParB-c3 to both cognate and noncognate *parS* sites (Fig. 6B, $c3_{A5K}$ lanes); (ii) replacement of Gly 9 of ParB-c3 by Asp, as in ParB-12D, or by Thr, as in ParB-12J, reduces binding to *parS* (Fig. 6B, $c3_{G9D}$ and $c3_{G9T}$ lanes); (iii) in contrast, replacement of Asp 9 by Gly in ParB-12D results in binding at least as strong as that with the wild type (Fig. 6B). Points ii and iii corroborate the role of Gly 9 in ParB-c3 as the highly conserved interhelix hinge residue of HTH motifs. Hence, although designation of these regions as HTH domains is provisional, we refer to them as such hereafter.

To analyze its role in centromere binding, we exchanged the whole HTH of ParB-c3, as depicted in Fig. 6A, for those of ParB-G4, -12J, and -12D. The three hybrid ParB-c3 proteins were produced at comparable concentrations (see Fig. S1 and Table S1 in the supplemental material) and were functional in the sense that they all bound to *parS*-c3 and *parS*-12J. ParB-$c3_{HTH-12J}$ binding is little impaired compared with that of ParB-c3, even though the amino acid changes include G9T, which by itself reduces binding strongly (Fig. 6B; compare lanes $c3_{G9T}$, $c3_{HTH-12}$, and c3), implying that the exchanged region acts as a functional unit. Nevertheless, no clear shift in binding specificity was seen with the G4 (data not shown) and 12J hybrids, suggesting that some determinants of specificity lie outside the HTH.

On the other hand, the binding characteristics of ParB-$c3_{HTH-12D}$ plainly differed from those of ParB-c3. While ParB-c3 bound each of the three *parS* probes to form the same pattern of three retarded bands, ParB-$c3_{HTH12D}$ formed a single complex with *parS*-12D which migrated like that formed with its cognate ParB, indicating a clear alteration in binding behavior associated with the exchange of putative HTH motifs. The change in specificity is partial, however, since like ParB-c3 but unlike ParB-12D, the 12D hybrid binds to the c3 and 12J *parS* sites. These results imply that in the Bsr3 group of ParB proteins, elements both inside and outside the putative HTH motif determine *parS* binding specificity.

DISCUSSION

Although the strong similarities among the Par systems of *B. cenocepacia* could lead one to expect that they interact, the results of all tests applied *in vivo* (stabilization in *E. coli* and growth inhibition in *B. cenocepacia*) and *in vitro* (EMSA) attest to their nonoverlapping specificities. It is rather in the taxonomic neighborhood of *B. cenocepacia* that we have discovered cross-reactions between Par systems allowing us to propose evolutionary relationships.

The Bsr families of *Burkholderiales* and their centromeres. To identify Par systems similar to those of *B. cenocepacia* J2315, we focused our analysis on the search for new centromeres. Livny et al. (39), using sequence matrices based on the chromosomal *parS* sites then known, revealed the wide distribution of such sites among bacterial species and replicons but identified no new centromere motifs. Our search was based on the centromere structure, i.e., palindromes of at least 14 bp with a central 5′-CG dinucleotide. It led to the identification of 8 new *parS* motifs, including one in *Rhodoferax ferrireducens* plasmid 1 (Bsr5-c [Fig. 3]) missed in the previous analysis. We brought to light seven families of such Par systems, all exclusive to secondary chromosomes and large plasmids of *Burkholderiales*, which by itself implies a phylogenetic

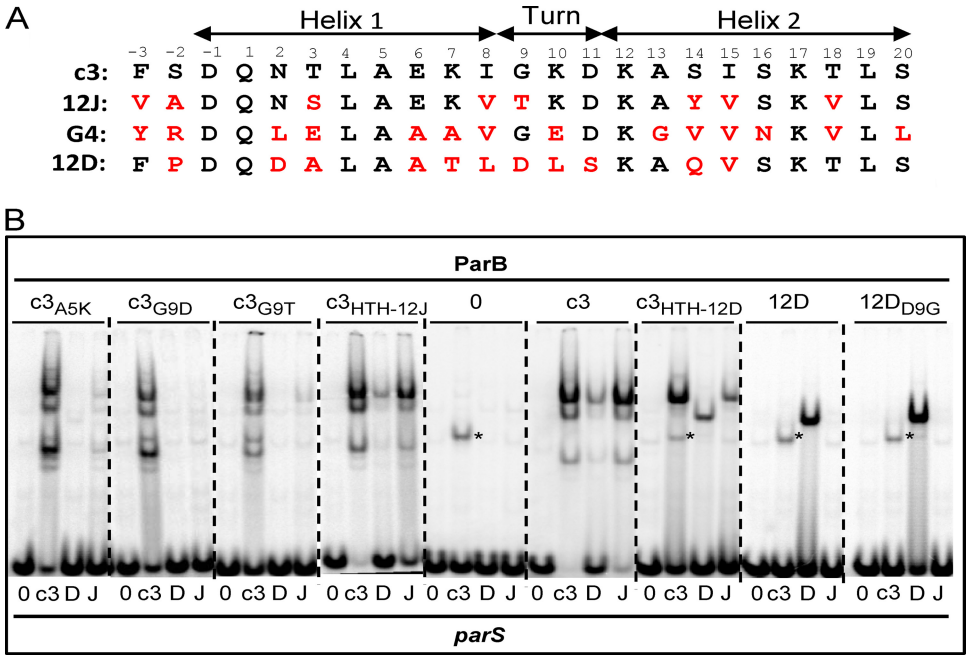

FIG 6 Modifications in a putative HTH domain of ParB-Bsr3. (A) Comparison of the putative HTH domains of ParB-c3, -12J, -G4, and -12D. Amino acids identical to ParB-c3 are in black, others in red. Positions are numbered and presumed helices are shown. (B) EMSA of ParB proteins with the HTH domain exchanged (from −3 to 20 according to the numbering in panel A) or modified as shown above each panel, e.g., for $c3_{A5K}$, ParB-c3 with Lys substituted for Ala at position 5. The *parS* probes are denoted below each lane as follows: 0, negative-control sequence CTAGTCGTACGACTAG; c3, *parS*-c3; D, *parS Ralstonia pickettii* 12D plasmid 1; J, main *parS Ralstonia pickettii* 12J. The *parS*-c3 fragment is also retarded by an unknown *E. coli* protein (*). Note that the three-band pattern typical of ParB-c3, possibly resulting from protein cleavage at sites distant from the HTH, is replaced by a single band after substitution with the 12D HTH. This exchange would not be expected to eliminate protease sensitivity of two sites, suggesting that the three-band pattern could have another explanation, such as formation by ParB-c3 of three types of complex with *parS* sites, each with a different gel electrophoretic mobility.

linkage. Incidentally, in the case of Bsr3-a, i.e., the Par subtype characteristic of the chromosome 3 of Bcc members, this feature could aid in identification of Bcc pathogens. For example, the pathogen *Burkholderia ubonensis*, classified with difficulty as a Bcc member because of an atypical phenotype (53), has the Bsr3-a subtype. Conversely, *Burkholderia xenovorans* has a third chromosome, like Bcc members, but does not belong to the Bcc and, accordingly, does not carry a Bsr3-a subtype.

A notable parallel to the Bsr family of Par systems is found in the *Rhizobiales*, whose secondary replicons and megaplasmids are characterized by loci (*repABC*) that combine both partition (RepAB, analogous to ParAB) and replication (RepC) functions (10). As in the Bsr families, the *parS* sites of RepAB families are palindromes of 16 bp with a T-rich 5′ end. The only prominent difference is that whereas the central dinucleotide in Bsr-*parS* sites is CG, in Rep-*parS* sites it is GC. *Rhizobiales* and *Burkholderiales* belong to different classes, *Alphaproteobacteria* and *Betaproteobacteria*, respectively, but are both remarkable for the frequency of species that exhibit division of their genome into large replicons. Although the advantage conferred by split genomes is unclear, the diversification of an ancestral partition system (Rep or Bsr) in compatible descendants would have been central to the stability of large secondary replicons.

Further analysis of the newly identified *parS* families reveals some interesting aspects. The internal 14 bp appears to be the essential component of *parS* palindromes: although palindromes may extend to 16 bp, positions 1 and 16 are naturally the most variable, and our tests of *parS*-c1 and *parS*-c3 *in vivo* and *in vitro* show that these positions are less important. On the other hand, the 6-bp core of Bsr centromeres varies less than could be expected on the basis of the core sequences of *B. cenocepacia* c2, c3, and pBC and of *Ralstonia solanacearum* c2, i.e., the models for our search for new centromeres. These sequences, TGCGCA, CACGTG, CTCGAG, and AGCGCT, respectively, all consist of 2 C's, 2 G's, 1 A, and 1 T (Table 1). Keeping the central CG and the palindromic structure, this base composition rule would predict four additional sequences: ACCGGT, GACGTC, GTCGAC, and TCCGGA. We found the core ACCGGT in the Bsr5 family (Fig. 3) but were unable to find the three other motifs within putative centromeres. Unless genomes containing such *parS* sites have not yet been sequenced, this result suggests tighter constraint on *parS* base composition. However, some families, e.g., Bsr5 and Bsr3, display clear variation in *parS* (border or core sequences) associated with ParB variants (Fig. 3). This observation suggests that an ancestral ParB-*parS* cognate pair may relax its specificity, coevolve, and generate a diversity of subtypes.

Binding of ParB-c3 to family centromeres: is it ancestral? The Bsr3 family includes four clearly distinct Par subtypes: C3 (chromosome 3 of J2315 and all Bcc members), G4 (*B. vietnamiensis* G4 plasmid 2), 12J (*R. pickettii* 12J plasmid integrated in chromosome 1), and 12D (*R. pickettii* 12D plasmid 1). Bsr3 appeared well-suited to testing ParB-*parS* cross-interaction within the family and to tracking a Par evolutionary pathway. In assessing which of these Par systems is closest to an ancestral form, we assume that an ancestor possesses the most general properties and that descendants acquire a more restricted binding specificity that allows

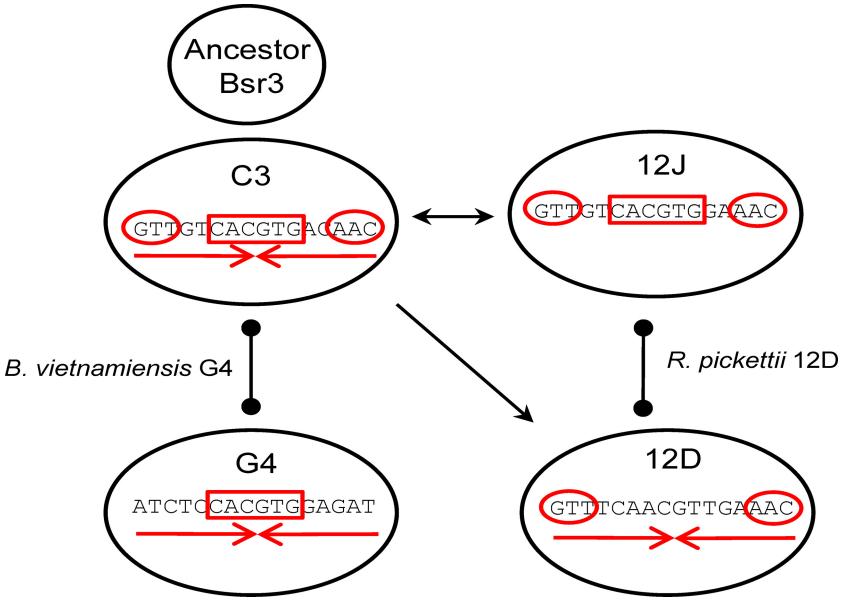

FIG 7 Evolution of an ancestral Bsr3-Par system. The Par system of *Burkholderia cepacia* complex chromosome 3 (C3) is proposed to be the most likely ancestor. Its ParB has a relatively wide binding specificity, and its *parS* comprises the features of the other systems: GTT ends (red circles), CACGTG core (red rectangle), and symmetry (red convergent arrows). An ancestral plasmid form would have been captured and frozen by C3 but would have spread on other plasmid replicons and diverged to generate the Par systems 12J, 12D, and G4, each with a *parS* having lost one feature. Where evolution has proceeded in different species, without the requirement for compatibility, ParB-*parS* cross-reaction can be detected (arrows). When managing two replicons in the same species (e.g., *B. vietnamiensis* G4 and *R. pickettii* 12D), Par systems must diverge for the replicons to be compatible and ParB-*parS* cross-reaction is detected barely or not at all (ball lines).

compatibility with other Par systems. G4 is an example of the latter. *B. vietnamiensis* G4 is a Bcc member, and as such, it carries a C3 system. Accordingly, G4 and C3 do not cross-react. Indeed, despite their common core, CACGTG, *parS*-G4 and *parS*-c3 differ by 8 bases, and the ParB-G4 and ParB-c3 HTH domains differ at many residues (Fig. 6A), suggesting evolution for compatibility between G4 and C3.

In contrast, there is no compatibility constraint between subtypes C3 and 12J or between C3 and 12D, C3 being from *Burkholderia*, the latter two from *Ralstonia*. We found indeed that ParB-c3 binds to *parS*-12J and, more weakly, to *parS*-12D. 12J has one arm of *parS* identical to one *parS*-c3 arm, and its ParB HTH is similar to that of C3 (Fig. 6A). These similarities explain the cross-reaction between 12J and C3. In contrast, the cross-reaction between 12D and C3, even though weak, is unexpected. The HTH domain of ParB-12D strongly diverges from that of ParB-c3 (Fig. 6A), and *parS*-12D differs from *parS*-c3 by three double changes (positions 4 to 6 and symmetric 11 to 13). Besides, one of these changes introduced alone in *parS*-c3 (positions 5 and 12 [Fig. 5]) almost completely abolished the binding to ParB-c3 (Fig. 5). It appears that binding of ParB-c3 to *parS*-12D is based not on mere residual affinity for a degenerate site but on the recognition of this *parS* in its entirety.

ParB-c3 is the least specialized of the Bsr3 proteins tested. Its HTH domain has an interhelix glycine, a feature of most HTHs which was adaptable here to the HTH of ParB-12D. In contrast, the HTH of ParB-12D has an atypical interhelix Asp, which prevents significant binding of the hybrid protein to noncognate *parS* sites, suggesting that the HTH domain of ParB-12D is more specialized. Besides, ParB-c3 binds noncognate *parS*, even the distantly related *parS*-12D. The frame of ParB-c3 is sufficiently adaptable to accommodate related DNA-binding domains in functional form. The swapped ParB-c3$_{HTH12D}$ even binds *parS*-12D, producing a single retarded species similar to that observed with ParB-12D (Fig. 6B). These observations argue for ParB-c3 as the ancestor of the Bsr3 group. Likewise, *parS*-c3, with its symmetrical form, core CACGTG, and terminal GTT, appears ancestral; each related *parS* has lost one of these features—12J the symmetry, 12D the core, and G4 the ends (see Fig. 7 for a summary).

Is a third chromosome emerging in *Ralstonia pickettii*? *R. pickettii* 12D carries not only a 12D Bsr3-Par subtype, on its plasmid 1, but also a 12J subtype, on its 270-kb plasmid 2. The latter is an exact copy—proteins, *parS* sequence, and repeat arrangement—of that found in *R. pickettii* 12J, on a 380-kb replicon integrated in c1. Remarkably, the 380-kb integrant of *R. pickettii* 12J

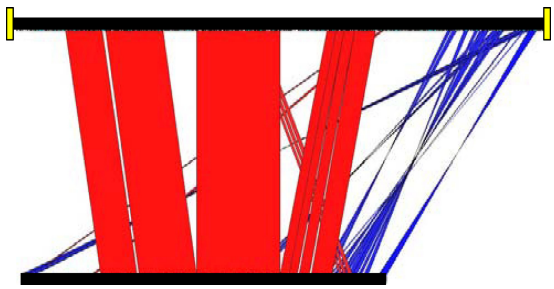

FIG 8 *Ralstonia pickettii* 12J chromosome 1 compared to *R. pickettii* 12D plasmid 2. *Ralstonia pickettii* 12J chromosome 1, nucleotides 1,560,000 to 1,950,000, is represented at the top, the whole *Ralstonia pickettii* 12D plasmid 2 at the bottom. They share extensive sequence homology and gene order. Conserved blocks with 99% identity are shown in red. Blue blocks correspond to inversions with sequence conservation above 80%. Duplications of 6 kb, presumably arising during plasmid integration, are highlighted as yellow blocks. (See also Materials and Methods.)

corresponds to the 270-kb plasmid 2 of *R. pickettii* 12D (Fig. 8), sharing with it blocks of DNA 99% identical. The integrant, however, has been enlarged to 380 kb by the acquisition of blocks of heterologous DNA. Presumably this accretion can continue, up to and beyond the eventual excision of the replicon. It is frequently proposed that secondary chromosomes are derived from plasmids by horizontal gene transfer and genome shuffling. We seem to be witnessing this situation in *R. pickettii* 12J. This strain is a melting pot from which a chromosome 3 is emerging, under the necessary constraints of a Par system (subtype 12J) that is most similar to the Par system (subtype C3) controlling chromosome 3 of the *Burkholderia cepacia* complex.

ACKNOWLEDGMENTS

We thank M. Arlat, D. Lovley, T. Marsh, and J. Tiedje for providing genomic DNA and strains of *Ralstonia solanacearum*, *Rhodoferax ferrireducens*, *Ralstonia pickettii* 12J and 12D, and *Burkholderia vietnamiensis* G4. We also thank the diligent reviewers whose remarks improved the manuscript. We are grateful to J.-Y. Bouet for advice on EMSA and to J. Rech for technical assistance and logistics.

This work was supported by ANR grant 06-BLAN-0280-01.

REFERENCES

1. **Altschul SF, et al.** 1997. Gapped BLAST and PSI-BLAST: a new generation of protein database search programs. Nucleic Acids Res. **25**:3389–3402.
2. **Balzer D, Ziegelin G, Pansegrau W, Kruft V, Lanka E.** 1992. KorB protein of promiscuous plasmid RP4 recognizes inverted sequence repetitions in regions essential for conjugative plasmid transfer. Nucleic Acids Res. **20**:1851–1858.
3. **Barillà D, Rosenberg MF, Nobbmann U, Hayes F.** 2005. Bacterial DNA segregation dynamics mediated by the polymerizing protein ParF. EMBO J. **24**:1453–1464.
4. **Bartosik AA, Jagura-Burdzy G.** 2005. Bacterial chromosome segregation. Acta Biochim. Pol. **52**:1–34.
5. **Bignell C, Thomas CM.** 2001. The bacterial ParA-ParB partitioning proteins. J. Biotechnol. **91**:1–34.
6. **Bouet J-Y, Ah-Seng Y, Benmeradi N, Lane D.** 2007. Polymerization of SopA partition ATPase: regulation by DNA binding and SopB. Mol. Microbiol. **63**:468–481.
7. **Campbell CS, Mullins RD.** 2007. In vivo visualization of type II plasmid segregation: bacterial actin filaments pushing plasmids. J. Cell Biol. **179**:1059–1066.
8. **Carver TJ, et al.** 2005. ACT: the Artemis Comparison Tool. Bioinformatics **21**:3422–3423.
9. **Castaing J-P, Bouet J-Y, Lane D.** 2008. F plasmid partition depends on interaction of SopA with non-specific DNA. Mol. Microbiol. **70**:1000–1011.
10. **Cevallos MA, Cervantes-Rivera R, Gutiérrez-Ríos RM.** 2008. The repABC plasmid family. Plasmid **60**:19–37.
11. **Chevenet F, Brun C, Bañuls A-L, Jacq B, Christen R.** 2006. TreeDyn: towards dynamic graphics and annotations for analyses of trees. BMC Bioinformatics **7**:439.
12. **Davis MA, Martin KA, Austin SJ.** 1990. Specificity switching of the P1 plasmid centromere-like site. EMBO J. **9**:991–998.
13. **Dsouza M, Larsen N, Overbeek R.** 1997. Searching for patterns in genomic data. Trends Genet. **13**:497–498.
14. **Dubarry N, Du W, Lane D, Pasta F.** 2010. Improved electrotransformation and decreased antibiotic resistance of the cystic fibrosis pathogen *Burkholderia cenocepacia* strain J2315. Appl. Environ. Microbiol. **76**:1095–1102.
15. **Dubarry N, Pasta F, Lane D.** 2006. ParABS systems of the four replicons of *Burkholderia cenocepacia*: new chromosome centromeres confer partition specificity. J. Bacteriol. **188**:1489–1496.
16. **Ebersbach G, Gerdes K.** 2001. The double par locus of virulence factor pB171: DNA segregation is correlated with oscillation of ParA. Proc. Natl. Acad. Sci. U. S. A. **98**:15078–15083.
17. **Egan ES, Fogel MA, Waldor MK.** 2005. Divided genomes: negotiating the cell cycle in prokaryotes with multiple chromosomes. Mol. Microbiol. **56**:1129–1138.
18. **Fothergill TJG, Barillà D, Hayes F.** 2005. Protein diversity confers specificity in plasmid segregation. J. Bacteriol. **187**:2651–2661.
19. **Funnell BE, Gagnier L.** 1993. The P1 plasmid partition complex at parS. II. Analysis of ParB protein binding activity and specificity. J. Biol. Chem. **268**:3616–3624.
20. **Gallie DR, Kado CI.** 1987. *Agrobacterium tumefaciens* pTAR *parA* promoter region involved in autoregulation, incompatibility and plasmid partitioning. J. Mol. Biol. **193**:465–478.
21. **Gerdes K, Møller-Jensen J, Bugge Jensen R.** 2000. Plasmid and chromosome partitioning: surprises from phylogeny. Mol. Microbiol. **37**:455–466.
22. **Gerdes K, Howard M, Szardenings F.** 2010. Pushing and pulling in prokaryotic DNA segregation. Cell **141**:927–942.
23. **Godfrin-Estevenon A-M, Pasta F, Lane D.** 2002. The *parAB* gene products of *Pseudomonas putida* exhibit partition activity in both *P. putida* and *Escherichia coli.* Mol. Microbiol. **43**:39–49.
24. **Gruber S, Errington J.** 2009. Recruitment of condensin to replication origin regions by ParB/SpoOJ promotes chromosome segregation in *B. subtilis.* Cell **137**:685–696.
25. **Guindon S, Gascuel O.** 2003. A simple, fast, and accurate algorithm to estimate large phylogenies by maximum likelihood. Syst. Biol. **52**:696–704.
26. **Hatano T, Yamaichi Y, Niki H.** 2007. Oscillating focus of SopA associated with filamentous structure guides partitioning of F plasmid. Mol. Microbiol. **64**:1198–1213.
27. **Holden MTG, et al.** 2009. The genome of *Burkholderia cenocepacia* J2315, an epidemic pathogen of cystic fibrosis patients. J. Bacteriol. **191**:261–277.
28. **Isles A, et al.** 1984. *Pseudomonas cepacia* infection in cystic fibrosis: an emerging problem. J. Pediatr. **104**:206–210.
29. **Jones DT, Taylor WR, Thornton JM.** 1992. The rapid generation of mutation data matrices from protein sequences. Comput. Appl. Biosci. **8**:275–282.
30. **Kadoya R, Baek JH, Sarker A, Chattoraj DK.** 2011. Participation of chromosome segregation protein ParAI of *Vibrio cholerae* in chromosome replication. J. Bacteriol. **193**:1504–1514.
31. **Katoh K, Kuma K, Toh H, Miyata T.** 2005. MAFFT version 5: improvement in accuracy of multiple sequence alignment. Nucleic Acids Res. **33**:511–518.
32. **Kim HJ, Calcutt MJ, Schmidt FJ, Chater KF.** 2000. Partitioning of the linear chromosome during sporulation of *Streptomyces coelicolor* A3(2) involves an *oriC*-linked *parAB* locus. J. Bacteriol. **182**:1313–1320.
33. **Larsen RA, et al.** 2007. Treadmilling of a prokaryotic tubulin-like protein, TubZ, required for plasmid stability in *Bacillus thuringiensis.* Genes Dev. **21**:1340–1352.
34. **Lee PS, Grossman AD.** 2006. The chromosome partitioning proteins Soj (ParA) and Spo0J (ParB) contribute to accurate chromosome partitioning, separation of replicated sister origins, and regulation of replication initiation in *Bacillus subtilis.* Mol. Microbiol. **60**:853–869.
35. **Lemonnier M, Bouet JY, Libante V, Lane D.** 2000. Disruption of the F plasmid partition complex in vivo by partition protein SopA. Mol. Microbiol. **38**:493–505.
36. **Lemonnier M, Lane D.** 1998. Expression of the second lysine decarboxylase gene of *Escherichia coli.* Microbiology **144**(Part 3):751–760.
37. **Leonard TA, Butler PJG, Löwe J.** 2004. Structural analysis of the chromosome segregation protein Spo0J from *Thermus thermophilus.* Mol. Microbiol. **53**:419–432.
38. **Lin DC, Grossman AD.** 1998. Identification and characterization of a bacterial chromosome partitioning site. Cell **92**:675–685.
39. **Livny J, Yamaichi Y, Waldor MK.** 2007. Distribution of centromere-like *parS* sites in bacteria: insights from comparative genomics. J. Bacteriol. **189**:8693–8703.
40. **Mahenthiralingam E, Urban TA, Goldberg JB.** 2005. The multifarious, multireplicon *Burkholderia cepacia* complex. Nat. Rev. Microbiol. **3**:144–156.
41. **Møller-Jensen J, Jensen RB, Löwe J, Gerdes K.** 2002. Prokaryotic DNA segregation by an actin-like filament. EMBO J. **21**:3119–3127.
42. **Morales VM, Bäckman A, Bagdasarian M.** 1991. A series of wide-host-range low-copy-number vectors that allow direct screening for recombinants. Gene **97**:39–47.
43. **Mori H, Kondo A, Ohshima A, Ogura T, Hiraga S.** 1986. Structure and

function of the F plasmid genes essential for partitioning. J. Mol. Biol. **192**:1–15.
44. **Murray H, Errington J.** 2008. Dynamic control of the DNA replication initiation protein DnaA by Soj/ParA. Cell **135**:74–84.
45. **Ogura T, Hiraga S.** 1983. Partition mechanism of F plasmid: two plasmid gene-encoded products and a cis-acting region are involved in partition. Cell **32**:351–360.
46. **Perrière G, Gouy M.** 1996. WWW-query: an on-line retrieval system for biological sequence banks. Biochimie **78**:364–369.
47. **Saint-Dic D, Frushour BP, Kehrl JH, Kahng LS.** 2006. A *parA* homolog selectively influences positioning of the large chromosome origin in *Vibrio cholerae.* J. Bacteriol. **188**:5626–5631.
48. **Schumacher MA.** 2008. Structural biology of plasmid partition: uncovering the molecular mechanisms of DNA segregation. Biochem. J. **412**:1.
49. **Simpson AE, Skurray RA, Firth N.** 2003. A single gene on the staphylococcal multiresistance plasmid pSK1 encodes a novel partitioning system. J. Bacteriol. **185**:2143–2152.
50. **Tang M, Bideshi DK, Park H-W, Federici BA.** 2007. Iteron-binding ORF157 and FtsZ-like ORF156 proteins encoded by pBtoxis play a role in its replication in *Bacillus thuringiensis* subsp. *israelensis*. J. Bacteriol. **189**:8053–8058.
51. **Tinsley E, Khan SA.** 2006. A novel FtsZ-like protein is involved in replication of the anthrax toxin-encoding pXO1 plasmid in *Bacillus anthracis.* J. Bacteriol. **188**:2829–2835.
52. **Toro E, Hong S-H, McAdams HH, Shapiro L.** 2008. Caulobacter requires a dedicated mechanism to initiate chromosome segregation. Proc. Natl. Acad. Sci. U. S. A. **105**:15435–15440.
53. **Vanlaere E, et al.** 2008. *Burkholderia latens* sp. nov., *Burkholderia diffusa* sp. nov., *Burkholderia arboris* sp. nov., *Burkholderia seminalis* sp. nov. and *Burkholderia metallica* sp. nov., novel species within the *Burkholderia cepacia* complex. Int. J. Syst. Evol. Microbiol. **58**:1580–1590.
54. **Waterhouse AM, Procter JB, Martin DMA, Clamp M, Barton GJ.** 2009. Jalview Version 2—a multiple sequence alignment editor and analysis workbench. Bioinformatics **25**:1189–1191.
55. **Wu M, et al.** 2011. Segrosome assembly at the pliable parH centromere. Nucleic Acids Res. **39**:5082–5097.
56. **Yamaichi Y, Niki H.** 2000. Active segregation by the *Bacillus subtilis* partitioning system in *Escherichia coli.* Proc. Natl. Acad. Sci. U. S. A. **97**:14656–14661.
57. **Yamaichi Y, Fogel MA, McLeod SM, Hui MP, Waldor MK.** 2007. Distinct centromere-like *parS* sites on the two chromosomes of *Vibrio* spp. J. Bacteriol. **189**:5314–5324.